An experimental study of symmetry lowering of analcime

Neo Sugano and Atsushi Kyono

Division of Earth Evolution Sciences, Graduate School of Life and Environmental Sciences, University of Tsukuba, 1-1-1 Tennodai, Tsukuba, Ibaraki, 305-8572, Japan

Corresponding author: A. Kyono
Email: kyono@geol.tsukuba.ac.jp
Phone: +81-29-853-7176
Fax: +81-29-853-7887
orcid.org/0000-0001-5419-390X

Abstract

Single crystals of analcime were hydrothermally synthesized from a gel of analcime composition at 200 °C for 24 h. They were grown up to 100 μm in size with typical deltoidal icositetrahedron habit. The chemical composition determined by EPMA and TG analyses was $Na_{0.84}(Al_{0.89}Si_{2.12})O_6 \cdot 1.04H_2O$. The single-crystal X-ray diffraction method was used to determine the symmetry and crystal structure of analcime. The analcime grown from a gel crystallized in cubic space group *Ia*3*d* with lattice parameter a = 13.713(3) Å. In the cubic analcime, Si and Al cations were totally disordered over the framework *T* sites with site occupancy of Si:Al = 0.6871:0.3129(14). The single crystals of analcime with cubic symmetry were hydrothermally reheated at 200 °C in ultrapure water. After the hydrothermal treatment for 24 h, forbidden reflections for the cubic *Ia*3*d* symmetry were observed. The reflection conditions led to an orthorhombic space group *Ibca* with lattice parameters a = 13.727(2) Å, b = 13.707(2) Å, and c = 13.707(2) Å. The unit-cell exhibits a slight distortion with $(a + b)/2 > c$, yielding a flattened cell along c. In the orthorhombic analcime, Al exhibited a site preference for *T*11 site, which shows that the Si/Al ordering over the framework *T* sites lowers the symmetry from cubic *Ia*3*d* to orthorhombic *Ibca*. After the hydrothermal treatment for 48 h, reflections corresponding to orthorhombic space group *Ibca* were observed as well. The lattice parameters were a = 13.705(2) Å, b = 13.717(2) Å, and c = 13.706(2) Å, retaining the flattened cell shape with $(a + b)/2 > c$. The Si and Al cations were further ordered among the framework *T* sites than the case of the hydrothermal treatment for 24h. As a consequence, the Si/Al ordering was slightly but significantly accelerated with increasing the hydrothermal treatment time. During the hydrothermal reaction, however, chemical compositions were almost unchanged. The site occupancies of Na over the extra-framework sites remained unaffected with the heating time; thus, the hydrothermal heating influences the degree of ordering of Si and Al over the framework *T* sites rather than that of Na among the extra-framework sites.

Keywords: Analcime, Single-crystal X-ray diffraction, Symmetry lowering, Si/Al ordering

Introduction

Analcime, ideal chemical formula $NaAlSi_2O_6 \cdot H_2O$, is formed in a variety of geological environments that span a wide range of temperature and pressure from ambient to magmatic conditions (Neuhoff et al. 2004). Analcime is known to occur as a primary mineral in igneous rocks, a hydrothermal mineral occurring in veins and miarolitic cavities, and a secondary mineral in sedimentary rocks or altered pegmatites (Gaines et al. 1997), but the occurrences still remain a question as to whether it is primary or secondary (formed from leucite) (Wilkinson 1977; Karlsson and Clayton 1991; Pearce 1993; Demeny et al. 1997; Prelević et al. 2004; Seryotkin and Bakakin 2008; Henderson et al. 2014). The crystal structure of analcime is composed of a three dimensional framework of SiO_4 and AlO_4 tetrahedra with the ANA-type topology (Baerlocher et al., 2007). The ANA framework includes four-, six-, and eight-membered rings of the tetrahedra in the structure. The ANA-type is a common framework groups, and the following six natural zeolites belong to the ANA structure: analcime $Na[AlSi_2O_6] \cdot H_2O$, pollucite $(Cs,Na)[AlSi_2O_6] \cdot nH_2O$, wairakite $Ca[Al_2Si_4O_{12}] \cdot 2H_2O$, leucite $K[AlSi_2O_6]$, ammonioleucite $(NH_4)[AlSi_2O_6]$, and hsianghualite $Li_2Ca_3[Be_3Si_3O_{12}]F_2$ (Coombs et al. 1997; Baerlocher et al., 2007). The maximum symmetry of the ANA framework is cubic with space group *Ia*3*d*, but naturally occurring analcimes possess at least four different symmetries: cubic space group *Ia*3*d*, tetragonal space group $I4_1/acd$, orthorhombic space group *Ibca*, and monoclinic space group $I2/a$ (Ferraris et al. 1972; Mazzi and Galli 1978; Hazen and Finger 1979; Pechar 1988; Anthony et al. 1995). In addition to these symmetries, rhombohedral is also theoretically possible (Takéuchi et al. 1979). The previous study led to a conclusion that the symmetry lowering results from strict discrimination between Si and Al cations in the tetrahedral (*T*) sites of the ANA framework (Mazzi and Galli 1978). The ordering of Si and Al in the framework has also been studied using solid-state NMR technique (Murdoch et al. 1988; Teertstra et al. 1994; Phillips and Kirkpatrick 1994; Kohn et al. 1995; Cheng et al. 2000; Kim et al. 2010). Consequently, the ordering of Si and Al can be responsible for the symmetry lowering of analcime from cubic *Ia*3*d* to orthorhombic *Ibca*. With compression, furthermore, the symmetry of analcime changes to triclinic space group $P\bar{1}$, which is driven by tetrahedral tilting (Gatta et al. 2006).

Although natural analcimes exhibit a wide range of symmetries, little studies have been performed to investigate how the Si and Al move over the framework *T* sites with temperature

and heating time. Here, we report an experimental study of symmetry lowering of analcime by using single-crystal X-ray diffraction method. This approach toward the symmetry change in analcime would be helpful for investigating the classical mineralogical and petrological question as to whether the analcime is primary or secondary.

Experimental methods

Hydrothermal experiment

Single crystals of analcime were hydrothermally synthesized from a gel of analcime composition. First, aluminium sulfate $Al_2(SO_4)_3$ (Wako special grade, Wako Pure Chemical Industries, Ltd., Japan) and sodium metasilicate nonahydrate $Na_2SiO_3 \cdot 9H_2O$ (purity > 98.0%, Wako Pure Chemical Industries, Ltd., Japan) were used as starting materials. They were stoichiometrically mixed and transferred into a Teflon container with ultrapure water (Wako Pure Chemical Industries, Ltd., Japan). It was placed in an electric oven (DRM320DA, Advantec Toyo Kaisha, Ltd., Japan) and subsequently heated at 200 ^{o}C with autogenic pressure. After 24h, it was quenched into cold water. The products were then filtered and thoroughly rinsed with distilled water. The sample obtained in this way was hydrothermally reheated at 200 ^{o}C in the ultrapure water for different duration, after which it was quenched into cold water. The recovered sample was filtered and thoroughly rinsed with distilled water. The morphology of the synthesized products was observed by a field emission scanning electron microscopy (JSM6330F, JEOL Ltd., Japan) with an acceleration voltage of 5 kV. Pt-Pd was deposited for conductive treatment by an ion-sputtering coater (E-1045, Hitachi High-Technologies Corporation, Japan) with current of 15 mA for 120 s.

EPMA and TG-DTA analyses

Qualitative and quantitative analyses were conducted by a hyperprobe field emission electron probe microanalyzer (EPMA) equipped with wavelength-dispersive X-ray spectrometers (JXA-8530F, JEOL Ltd., Japan). Regarding EPMA analysis of hydrous alkali aluminosilicates, a long-standing problem is sample damage caused by the electron-beam, which is ascribed to the migration of Na and other alkalis. The migration is known to be permanent and irreversible after irradiation ceases (Autefage and Couderc 1980). The alkali

losses can be minimized with the use of carefully selected operating conditions. In the present study, to prevent the loss of Na*K*α X-ray intensity during electron-beam irradiation, measurements were performed under the experimental conditions based on the recommendation of Morgan and London (1996, 2005) and on the recent study of natural zeolites (Campbell et al. 2016). In the study, the X-ray spectra were thus measured using a beam diameter of 20 μm, an accelerating voltage of 15 kV, and a beam current of 2 nA with an acquisition time of 30 s on both the peak and background. Quartz (Si*K*α), corundum (Al*K*α), and albite (Na*K*α) were used as standards. No other elements were detected in the qualitative analyses. Raw data obtained were corrected using a conventional ZAF program. The chemical formulae of analcime were finally determined based on six oxygen atoms per formula unit (apfu).

In the study, thermogravimetry (TG) measurements were performed to obtain a reliable water content of analcime. Thermogravimetric (TG) and differential thermal analyses (DTA) were carried out with a TG/DTA thermal analyzer (EXTRA7000 TG/DTA7300, Seiko Instruments Inc., Japan). The samples of approximately 10 mg were mounted on an aluminum pan and heated under Ar gas flow of 200 ml/min. The temperature was increased from 55 ^{o}C to 550 ^{o}C at a heating rate of 10 ^{o}C/min. Al_2O_3 powder was used for the reference. As the previous studies had also indicated (Kim and Kirkpatrick 1998; Cruciani and Gualtieri 1999; Chipera and Bish 2010), the present TG-DTA measurement showed that analcimes kept 100% H_2O content until 100 ^{o}C and were completely dehydrated by 450 ^{o}C. The numbers of H_2O molecule per formula unit were therefore estimated by weight loss between 100 ^{o}C and 450 ^{o}C. The chemical composition of analcimes determined by EPMA and TG analyses are listed in Table 1.

Single-crystal X-ray diffraction study

For the single-crystal X-ray diffraction measurement, suitable single crystals were selected under a microscope. They were fixed at the top of 0.1 mm diameter glass fibers and mounted on a goniometer head. X-ray diffraction measurements were performed by using a single-crystal diffractometer (APEXII ULTRA, Bruker AXS Inc., Germany) equipped with a CCD detector, multilayer optics, and graphite monochromated Mo*K*α radiation (λ = 0.71073 Å) generated by a rotating anode. The sample-to-detector distance was set to 60 mm. A preliminary 36 frames of two dimensional diffraction images were collected and processed to

obtain the cell parameters and orientation matrix. A total of 720 frames covering a hemisphere of reciprocal space were collected with a step size of 0.5° in ω at three different φ setting (0, 90, 180°) and detector position of -28° in 2θ. The exposure time was 10 s per frame. Intensity data were integrated and corrected for Lorentz-polarization effects using the APEX2 software (Bruker 2006). Empirical absorption correction was also applied using the SADABS software (Sheldrick 1999). The space group symmetries were determined from the systematic absences. The structures were solved by a combination of the direct method and the difference Fourier methods provided by the program package SHELXTL (Bruker 1998). Unique reflections with $F_o > 4\sigma(F_o)$ were used in the structure refinements. Site occupancy parameters of Si and Al on the framework *T* sites were refined under a constraint that the total populations on each *T* site were unity, whereas those of Na cations were refined without any constraint. The crystal structures were finally refined by full matrix least-square methods on F^2 using SHELXL97 software (Sheldrick 1997). Since hydrogen atoms were not included in the calculations, water molecules were refined as oxygen atoms in the refinements. All atoms were refined on the basis of anisotropic displacement model. The crystallographic data, data collection, and structure refinement details are shown in Table 2. The refined structural parameters are given in Table 3. Selected bond distances are summarized in Table 4.

Results and Discussion

Chemical composition

Euhedral single crystals with the size up to approximately 100 μm were obtained from the gel. The single crystals grown in the study exhibited typical deltoidal icositetrahedron habit (Fig. 1a). The chemical compositions of as-grown analcime and its hydrothermally reheated samples are given in Table 1. The results of EPMA measurement show that the single crystals are chemically homogeneous and close to the ideal chemical composition of analcime. The totals of tetrahedral cations are approximately 3.00 atoms per formula unit (apfu), but the contents of Si ranges between 2.10 and 2.15 apfu. The contents of Na are, on the other hand, about 0.85 apfu, which is considerably less than the ideal value. The deficiencies of Na in extra-framework sites result from the excess positive charge on the framework caused by the excess Si. If the contents of H_2O molecule are estimated by the deficit of the total oxide weight from

100 wt%, they are ranged from 10.2 to 11.2 wt%. They correspond to 1.26 to 1.39 molecules per formula unit. The estimations are much higher than the ideal value of 1.00 molecule per formula unit. As Deer et al. (2004) have already pointed out, estimating water content by difference from 100 wt% by EPMA measurement never yield useful results. Thus, we determined the water contents in analcime by the thermogravimetry (TG) curves. In the present study, the weight losses between 100 and 450 ^{o}C were 8.4 wt%, which correspond to 1.03 to 1.04 molecules per formula unit. The H_2O contents obtained from the TG analysis are thus consistent approximately with the ideal value.

Putnis et al. (2007) reported that in hydrothermal reaction between analcime and leucite replacement of leucite by analcime proceeds by both dissolution of leucite and reprecipitation of analcime. They exhibited the SEM image showing crystal surfaces which are covered with the rough and porous surface layers of analcime. In the present study, however, no surface features indicating the dissolution and reprecipitation process were produced by the hydrothermal treatment (Fig. 1b, d). The most noteworthy feature in the present study is that the concentrations of Na, Al, and Si almost remained unchanged with increasing the hydrothermal heating time up to at least 48h.

As-grown analcime with cubic symmetry

No forbidden reflections for the cubic *Ia*3*d* symmetry were observed in the analcime grown from gel. The as-grown analcime therefore crystallized in cubic space group *Ia*3*d* with lattice parameter a = 13.713(3) Å (Table 2). The lattice parameter was slightly larger than that of naturally occurring cubic analcime, a = 13.7065(8) Å, with a chemical formula of $(Na_{0.887}K_{0.001}Ca_{0.001})(Al_{0.905}Si_{2.102})O_6 \cdot 0.994H_2O$ (Gatta et al. 2006). In the cubic analcime with the space group *Ia*3*d*, the framework *T* site is located on 48*g* Wyckoff positions, and hence 48 tetrahedra are symmetrically equivalent. The framework *T* site is randomly occupied with site occupancy of Si:Al = 0.6871:0.3129(14) (Table 3). The *T*-O bond lengths ranging from 1.6430(11) to 1.6465(11) Å (Table 4) agree well with the values reported in the previous study (Gatta et al. 2006). The *T*-O bond lengths are an indicator of Si/Al disordering. Wairakite belongs to a group of minerals with the ANA-type framework topology and has a fully ordered Si/Al distribution (Takéuchi et al. 1979; Seryotkin et al. 2003). The completely ordered Si-O and Al-O bond lengths in wairakite are in the ranges of 1.604 to 1.617 Å and of 1.730 to 1.731 Å, respectively (Seryotkin et al. 2003). We established a regression line between the completely

ordered Si-O and Al-O bond lengths as follows: *T*-O bond length (Å) = 0.1215×*SOP*(Al) + 1.609 (R^2 = 0.9952), where *SOP*(Al) is the site occupancy parameter of Al. Assuming that the *T*-O bond lengths reflect only Al content, the average *T*-O bond length of 1.645 Å obtained in our study corresponds to the Al site occupancy parameter of 0.2963. This estimation is very close to the refined site occupancy parameter of Al [= 0.3129(14); Table 3]. Analcime, ideal chemical formula $NaAlSi_2O_6 \cdot H_2O$, contains 16 formula units in the unit-cell. In the cubic space group *Ia*3*d*, Na is located on the Wyckoff positions 24*c* with multiplicity 24. The maximum site occupancy of Na is therefore 16/24. In the present study, the resulting site occupancy parameter of Na is 0.6040(14) (Table 3), implying that the number of Na corresponds to 0.906 apfu. As a result, the chemical formula obtained from the site occupancy parameters is $Na_{0.906}(Al_{0.939}Si_{2.061})O_6 \cdot H_2O$, which is similar to that of the naturally occurring cubic analcime (Gatta et al. 2006). In the analcime, Na cation is octahedrally coordinated by four framework oxygen atoms and two water molecules. The Na-O bond lengths were longer than the Na-*W* bond lengths (Table 4). The longer Na-O bond lengths arise from the deficiency of Na in the extra-framework sites (Mazzi and Galli 1978). Compared with the Na-O and Na-*W* bond lengths refined by Gatta et al. (2006), they are entirely consistent with the values obtained in the present study. The chemical formula obtained from the EPMA and TG analyses is, on the other hand, $Na_{0.84}(Al_{0.89}Si_{2.12})O_6 \cdot 1.04H_2O$ (Table 1). The chemical characteristic of excess Si and deficiencies of Na and Al is in good agreement with the result of crystal structural analysis. Taking the structural and chemical similarities into consideration, there is no significant difference between naturally occurring analcime and analcime hydrothermally grown in the present study.

According to the previous paper (Coombs et al. 1997), the basic structure of zeolite is an aluminosilicate framework composed of SiO_4 and AlO_4 tetrahedra. The framework is negatively charged and attracts the positive cations in the open cages. The negative charge of the framework results from the substitution of Si^{4+} by Al^{3+}, which is compensated by alkaline cations. With increasing the Si/Al ratio in the framework, the Na and Al contents decrease, but the H_2O content increases. In the cubic analcime, a Na atom is octahedrally coordinated with four framework oxygens with Na-O distance of 2.5007(12) Å and two water molecules with Na-W distance of 2.4241(5) Å. Water molecules are, on the other hand, located at the center of the wide cages of the framework structure. The H_2O molecule is connected not only to the Na but also to the framework oxygens with weak hydrogen bonding. There are six hydrogen bonds

between the water molecule and framework oxygen with W⋯O distance of 3.4055(14) Å and the other six hydrogen bonds with W⋯O distance of 3.5584(14) Å. The H_2O molecules are surrounded by the 12 weak hydrogen bonds in the wide cages. Therefore, even if the Na polyhedron is lost from the cage, the water molecule can remain around the center of cage with the hydrogen bond. The Na deficiency is fairly common in analcime (e.g., Pechar 1988, Line et al. 1995, Cruciani and Gualtieri 1999, Neuhoff et al. 2004, Gatta et al. 2006, Campbell et al. 2016), but the number of H_2O molecules never decreases with decreasing the Na content.

Symmetry lowering by Si/Al ordering with hydrothermal treatment

After the hydrothermal treatment of analcime at 200 ºC for 24h, weak reflections of type 00*l* with *l* = 2*n* became observed, which correspond to the reflection conditions of orthorhombic *Ibca*. When a phase transformation is examined from reflection conditions, the greatest care should be given to the multiple diffraction because the observation of the multiple diffraction spots often lead to an incorrect space group. We carefully checked the symmetrically equivalent reflections of 00*l* reflections with *l* = 2*n* and analyzed their intensity profiles over the rocking angle. In the present study, the equivalent reflections 0010 and $00\overline{1}0$ were examined and their intensity profiles are shown in Figure 2. Comparing between both the reflections, the shapes of the two intensity profiles are almost identical. Furthermore, the intensity profiles over the rocking angle and their least-squares curves fitted to a Gaussian function are shown in Figure 2c and 2d. The Gauss areas, corresponding to the integrated intensities, of 0010 and $00\overline{1}0$ reflections are 321.3 and 310.7, respectively; the difference between both is only 3.3%. Since the intensity profile of both the reflections are thus very close, it is unlikely that they were caused by the multiple diffraction. Therefore, we concluded from the appearance of the 00*l* reflections with *l* = 2*n* that symmetry of the analcime changes to orthorhombic *Ibca* with the hydrothermal treatment for 24h.

The lattice parameters refined with the orthorhombic cell were *a* = 13.727(2) Å, *b* = 13.707(2) Å, and *c* = 13.707(2) Å (Table 2). The unit-cell exhibits a slight distortion with (*a* + *b*)/2 > *c*, yielding a flattened cell along *c*. With the symmetry lowering of cubic analcime, crystallographically equivalent positions are split into inequivalent positions (Fig. 3). In the cubic *Ia*3*d*, the framework *T* site and extra-framework Na site are located on 48*g* and 24*c* Wyckoff positions, respectively. The *W* site is on 16*b* Wyckoff positions. As it can be seen in Figure 3b, with symmetry lowering to the tetragonal $I4_1/acd$, the framework *T* site on 48*g* is

split into the *T*1 site on 32*g* and *T*2 site on 16*f*. The Na site on 24*c* is split into Na1 site on 16*e* and Na2 site on 8*b*. The *W* site on 16*b* is transformed to 16*f*. With further symmetry lowering to the orthorhombic *Ibca* (Fig. 3c), the *T*1 site on 32*g* is split into *T*11 and *T*12 sites on 16*f*. The Na1 site on 16*e* is split into Na11 on 8*c* and Na12 on 8*d*. The Na2 site on 8*b* is transformed to 8*e*. With the hydrothermal treatment for 24 h, Si and Al cations in the orthorhombic phase showed a slightly ordered distribution over the three framework *T* sites with site occupancy of Si:Al = 0.618:0.382(2) on *T*11, 0.681:0.319(2) on *T*12, and 0.687:0.313(2) on *T*2 (Table 3). The most important feature in the present study is that Al exhibits a site preference for *T*11 site in the orthorhombic phase. Mazzi and Galli (1978) reported that the degree of unit-cell distortion in analcime depends on the Al fraction in the *T* sites: the flattened cell is caused by a higher Al fraction in *T*1 site, whereas the elongated cell is by a higher Al fraction in *T*2 site. This trend is entirely consistent with the case of the present orthorhombic analcime with the Al preference for *T*11 site derived from the tetragonal *T*1 site. The *T*11-O, *T*12-O and *T*2-O bond lengths are in the ranges of 1.6414(15) to 1.6477(16) Å, 1.6408(15) to 1.6463(16) Å, and 1.6411(15) to 1.6457(16) Å, respectively (Table 4). Despite the Al ordering in the *T* sites, thus, we could detect no significant difference in the *T*-O bond length among the *T*11, *T*12, and *T*2 sites. Site occupancies of Na11, Na12, and Na2 were 0.591(2), 0.598(2), and 0.596(2), respectively (Table 3). Na exhibits no significant site preference among the three Na sites, which is a similar feature to the naturally occurring analcime (Mazzi and Galli 1978). In the octahedral coordination of Na sites, the Na-O and Na-*W* bond lengths almost remain unchanged with the hydrothermal treatment for 24 h. As-grown analcime, hydrothermally formed from gel at 200 ^{o}C for 24h, might be frozen as the metastable cubic phase. With the additional heating time for 24h, the analcime would reach to the equilibrium state to change into the stable orthorhombic phage.

After the hydrothermal treatment for 48 h, reflections of type 0 0 *l* with $l = 2n$ appeared as well, which is consistent with the orthorhombic space group *Ibca*. The observed forbidden reflections were examined in the same way as the case of the hydrothermal treatment for 24h; consequently, they were concluded to be not due to the multiple diffraction. Lattice parameters with orthorhombic cell were a = 13.705(2) Å, b = 13.717(2) Å, and c = 13.706(2) Å, which retains the flattened cell shape with $(a + b)/2 > c$. The refined site occupancy parameters for Si and Al are Si:Al = 0.603:0.397(6) on *T*11, 0.694:0.306(6) on *T*12, and 0.687:0.313(6) on *T*2 (Table 3). With the hydrothermal treatment for 48 h, Al is further concentrated into *T*11 site. It is noteworthy that the Si/Al ordering was slightly but significantly accelerated with the

hydrothermal treatment time. The *T*11-O, *T*12-O, and *T*2-O bond lengths are in the ranges of 1.6416(14) to 1.6460(15) Å, 1.6415(14) to 1.6458(15) Å, and 1.6424(15) to 1.6467(15), respectively (Table 4). Thus, there is no significant difference in the *T*-O bond length among the *T*11, *T*12, and *T*2 sites, as well as the case of the hydrothermal treatment for 24h. The site occupancies in Na11, Na12, and Na2 sites are 0.594(2), 0.602(2), and 0.600(2), respectively (Table 3), which indicates that there is no significant site preference of Na cation over the three extra-framework sites, as well as the analcime hydrothermally heated for 24 h. During the hydrothermal reaction, chemical compositions were consequently almost unchanged. Since the site occupancies of Na over the extra-framework sites remained unaffected with increasing the heating time, the result shows that the heating time influences the degree of ordering of Si and Al over the framework *T* sites.

Two ordering models can be considered for the Si/Al ordering in the framework *T* sites. The first case is that the ordering gives rise to a site splitting of a *T* site into two crystallographycally inequivalent sites. In the present study, we experimentally confirmed the symmetry lowering of analcime induced by Si/Al ordering among the framework *T* sites. The second case is that the ordering proceeds continuously within the *T* sites, keeping the symmetry. Tetragonal analcimes with highly ordered Si/Al distribution in the *T* sites have been already reported (Mazzi and Galli 1978; Cruciani and Gualtieri 1999). In the tetragonal analcime, one edge of tetrahedron of *T*1 site shares with that of octahedron of Na site. Therefore, Mazzi and Galli (1978) exhibited that there is a direct relationship between Na occupancy and Al fraction in the nearest *T*1 site. That is to say, the highly ordered Si/Al distribution among the *T* sites must be caused by the high occupancy of Na in the extra-framework sites. In our experiment, as-grown cubic analcime was hydrothermally heated with ultrapure water in the Teflon container. During the hydrothermal treatment, no additional sodium source was supplied in the solution. This would be the reason why the Si/Al ordering was not drastically accelerated with the hydrothermal reaction. In other word, analcime with highly ordered Si/Al distribution among the *T* sites might be formed, when it is reheated under Na-rich solution.

CONCLUSIONS

In the study, a symmetry lowering of analcime from cubic *Ia*3*d* to orthorhombic *Ibca* was experimentally confirmed. With the hydrothermal treatment at 200 ^{o}C for 24 h, Al in the

framework *T* site is preferentially concentrated into *T*11 site, which yields three inequivalent *T* sites. The site splitting leads to the symmetry lowering from cubic *Ia*3*d* to orthorhombic *Ibca*. During the hydrothermal treatment, chemical composition was almost unchanged. Since Si/Al ordering was slightly but significantly accelerated with heating time, whereas the site occupancies of Na over the extra-framework sites remained unaffected with heating time. Thus, the result clearly shows that the heating time influences the degree of ordering of Si and Al over the framework *T* sites rather than that of Na among the extra-framework sites.

ACKNOWLEDGMENTS

We appreciate the incisive reviews by Akihiko Nakatsuka and an anonymous reviewer, which led to numerous improvements in the manuscript. We also thank Taku Tsuchiya for his editorial handling. The work was partially supported by a Grant-in-Aid for Scientific Research (C) from the Japan Society for the Promotion of Science (project no. 26400511).

REFERENCES

Anthony JW, Bideaux RA, Bladh KW, Nichols MC (1995) Handbook of mineralogy. vol. II, Silica, silicates, part 1, pp. 446, Mineral Data Publishing, Tucson, Arizona

Autefage F, Couderc J-J (1980) Étude du mécanisme de la migration du sodium et du potassium au cours de leur analyse à la microsonde électronique. Bull de Minéral 103:623–629

Baerlocher CH, McCusker LB, Olson DH (2007) Atlas of zeolite framework types. pp.398, Elsevier, Amsterdam

Bruker (1998) SHELXTL: structure determination programs Ver. 5.16. Bruker AXS Inc., Madison, Wisconsin, USA

Bruker (2006) Apex2 Version 2; Data collection and processing software. Bruker AXS Inc., Madison, Wisconsin, USA

Campbell LS, Charnock J, Dyer A, Hillier S, Chenery S, Stoppa F. Henderson CMB, Walcott R, Rumsey M (2016) Determination of zeolite-group mineral compositions by electron probe microanalysis. Mineral Mag 80:781–807

374 Cheng X, Zhao PD, Stebbins JF (2000) Solid state NMR study of oxygen site exchange and Al-
375 O-Al site concentration in analcime. Am Mineral 85:1030–1037
376 Chipera, SJ, Bish, DL (2010) Rehydration kinetics of a natural analcime. Eur J Mineral
377 22:787–795
378 Coombs DS, Alberti A, Armbruster T, Artioli G, Colella C, Galli E, Grice JD, Liebau F,
379 Mandarino JA, Minato H, Nickel EH, Passaglia E, Peacor DR, Quartieri S, Rinaldi
380 R, Ross M, Sheppard RA, Tillmanns E, Vezzalini G (1997) Recommended
381 nomenclature for zeolite minerals: Report of the Subcommittee on Zeolites of
382 International Mineralogical Association, Commission on New Minerals and
383 Minerals Names. Can Mineral, 35:1571–1606
384 Cruciani G, Gualtieri A (1999) Dehydration dynamics of analcime by in situ synchrotron
385 powder diffraction. Am Mineral 84:112–119
386 Deer WA, Howie RA, Wise WS, Zussman J (2004) Rock-Forming Minerals, 4B Framework
387 silicates - silica minerals, feldspathoids and zeolites. 982 p. The Geological Society,
388 London
389 Demeny A, Harangi S, Forizs I, Nagy G (1997) Primary and secondary features from analcimes
390 formed in carbonate-zeolite ocelli of alkaline basalts (Mecsek Mts., Hungary):
391 textures, chemical and oxygen isotope compositions. Geochem J 31:37–47
392 Ferraris G, Jones DW, Yerkess J (1972) A neutron-diffraction study of the crystal structure of
393 analcime, $NaAlSi_2O_6 \cdot H_2O$. Z Kristallogr 135:240–252
394 Gaines RV, Skinner HCW, Foord EE, Mason B, Rosenzweig A (1997) Dana's new mineralogy:
395 the system of mineralogy of James Dwight Dana and Edward Salisbury Dana. 8th
396 ed., pp 854, Wiley, New York
397 Gatta GD, Nestola F, Ballaran TB (2006) Elastic behavior, phase transition, and pressure
398 induced structural evolution of analcime. Am Mineral 91:568–578
399 Hazen RM, Finger LW (1979) Polyhedral tilting: A common type of pure displacive phase
400 transition and its relationship to analcime at high pressure. Phase Transitions, 1:1–22
401 Henderson CMB, Hamilton DL, Waters JP (2014) Phase equilibria in $NaAlSiO_4$-$KAlSiO_4$-
402 SiO_2-H_2O at 100 MPa pressure: equilibrium leucite composition and the enigma of
403 primary analcime in blairmorites revisited. Mineral Mag 78:171–202
404 Karlsson HR, Clayton RN (1991) Analcime phenocrysts in igneous rocks: primary or
405 secondary? Am Mineral 76:189–199

406 Kim Y, Kirkpatrick RJ (1998) High-temperature multi-nuclear NMR investigation of analcime.
407 Am Mineral 83:339–347
408 Kim Y, Lee SK, Kirkpatrick RJ (2010) Effects of intermediate range structure on the Si-29
409 NMR chemical shifts of framework silicates: Results for analcime. Am Mineral
410 95:1694–1700
411 Kohn SC, Henderson CMB, Dupree, R (1995) Si-Al order in leucite revisited: New information
412 from an analcite-derived analogue. Am Mineral 80:705–714
413 Line CM, Purnis A, Purnis C, Giampaolo C (1995) The dehydration kinetics and microtexture
414 of analcime from two parageneses. Am Mineral, 80:268–279
415 Mazzi F, Galli E (1978) Is each analcime different? Am Mineral 63:448–460
416 Morgan GB, London D (1996) Optimizing the electron microprobe analysis of hydrous alkali
417 aluminosilicate glasses. Am Mineral 81:1176–1185
418 Morgan GB, London D (2005) Effect of current density on the electron microprobe analysis of
419 alkali aluminosilicate glasses. Am Mineral 90:1131–1138
420 Murdoch JB, Stebbins JF, Carmichael ISE, Pines A (1988) A silicon-29 nuclear magnetic
421 resonance study of silicon-aluminum ordering in leucite and analcite. Phys Chem
422 Miner 15:370–382
423 Neuhoff PS, Hovis GL, Balassone G, Stebbins JF (2004) Thermodynamic properties of
424 analcime solid solutions. Am J Sci 304:21–66
425 Pearce TH (1993) Analcime phenocrysts in igneous rocks: primary or secondary? –discussion.
426 Am Mineral 78:225–229
427 Pechar F (1988) The crystal structure of natural monoclinic analcime ($NaAlSi_2O_6 \cdot H_2O$). Z
428 Kristallogr 184:63–69
429 Phillips BL, Kirkpatrick RJ (1994) Short-range Si-Al order in leucite and analcime:
430 Determination of the configurational entropy from ^{27}Al and variable-temperature
431 ^{29}Si NMR spectroscopy of leucite, its Cs- and Rb-exchanged derivatives, and
432 analcime. Am Mineral 79:1025-1031
433 Prelević D, Foley SF, Cvetkovic V, Romer RL (2004) The analcime problem and its impact on
434 the geochemistry of ultrapotassic rocks from Serbia. Mineral Mag 68:633–648
435 Putnis CV, Geisler T, Schmid-Beurmann P, Stephan T, Giampaolo C (2007) An experimental
436 study of the replacement of leucite by analcime. Am Mineral 92:19–26
437 Seryotkin YV, Joswig W, Bakakin VV, Belitsky IA, Fursenko BA (2003) High-temperature

crystal structure of wairakite. Eur J Mineral 15:475–484

Seryotkin YV, Bakakin VV (2008) The thermal behavior of secondary analcime as leucite derivate and its structural interpretation. Russ Geol Geophys 49:153–158

Sheldrick GM (1997) SHELXL97: Program for the refinement of crystal structures. University of Göttingen, Germany

Sheldrick GM (1999) SADABS: Empirical absorption and correction software. University of Göttingen, Germany

Takéuchi Y, Mazzi F, Haga N, Galli E (1979) The crystal structure of wairakite. Am Mineral 64:993–1001

Teertstra DK, Sherriff BL, Xu Z, Cerny P (1994) MAS and DOR NMR study of Al-Si order in the analcime-pollucite series. Can Mineral 32:69–80

Wilkinson JFG (1977) Analcime phencrysts in a vitrophyric analcimite–primary or secondary? Contrib Mineral Petrol 64:1–9

Captions for Figures and Tables

Figure 1 Field emission scanning electron microscope photographs of the hydrothermally synthesized analcime single-crystals. (a) As-grown sample with the deltoidal icositetrahedron habit and (b) magnified image of the area indicated by the square in (a). (c) Sample after additional hydrothermal treatment at 200°C for 24 h and (d) magnified image of the area indicated by the square in (c).

Figure 2 Intensity profiles recorded by CCD detector. (a) 0010 and (b) $00\overline{10}$ reflections corresponding to reflection conditions of type 00*l* with *l* = 2*n*, which is consistent with the orthorhombic space group *Ibca*. The rocking curves of the (c) 0010 and (d) $00\overline{10}$ reflections and their profiles fitted to a Gaussian function.

Figure 3 The six-membered ring channel and extra-framework species of analcime viewed along the [111] direction. The site splitting from (a) the cubic analcime with space group *Ia*3*d* to (c) the orthorhombic analcime with space group *Ibca* through (b) the tetragonal space group $I4_1/acd$. The terms in the parentheses denote Wyckoff positions.

Table 1 Representative chemical compositions of analcimes

Table 2 Selected X-ray diffraction data and crystallographic information for analcimes.

Table 3 Atomic coordinates, site occupancy parameters, equivalent isotropic, and anisotropic displacement parameters (Å^2).

Table 4 Selected bond lengths (Å) in framework *T* sites and extra-framework sites.

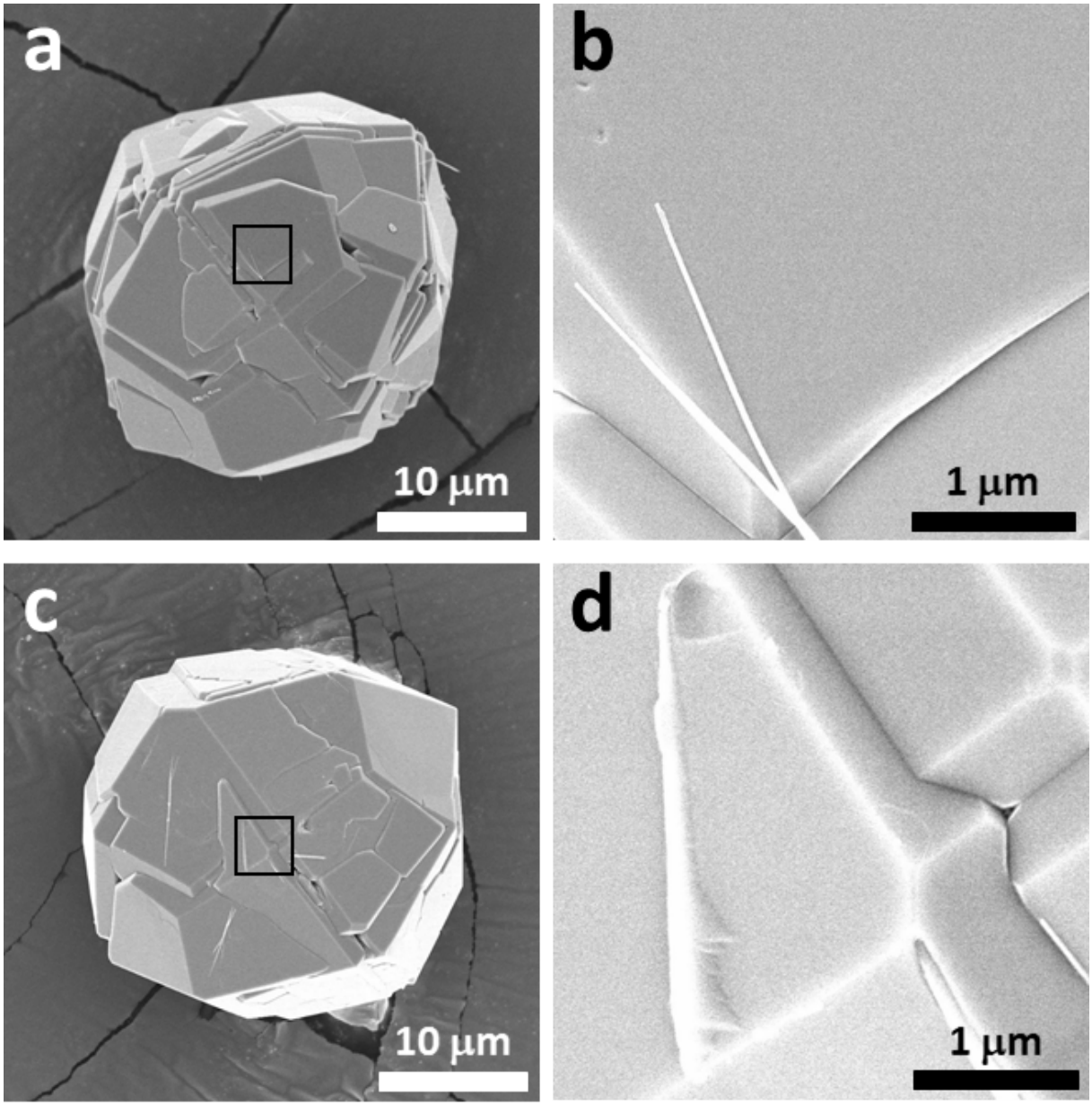

Figure 1 Field emission scanning electron microscope photographs of the hydrothermally synthesized analcime single-crystals. (a) As-grown sample with the deltoidal icositetrahedron habit and (b) magnified image of the area indicated by the square in (a). (c) Sample after additional hydrothermal treatment at 200°C for 24 h and (d) magnified image of the area indicated by the square in (c).

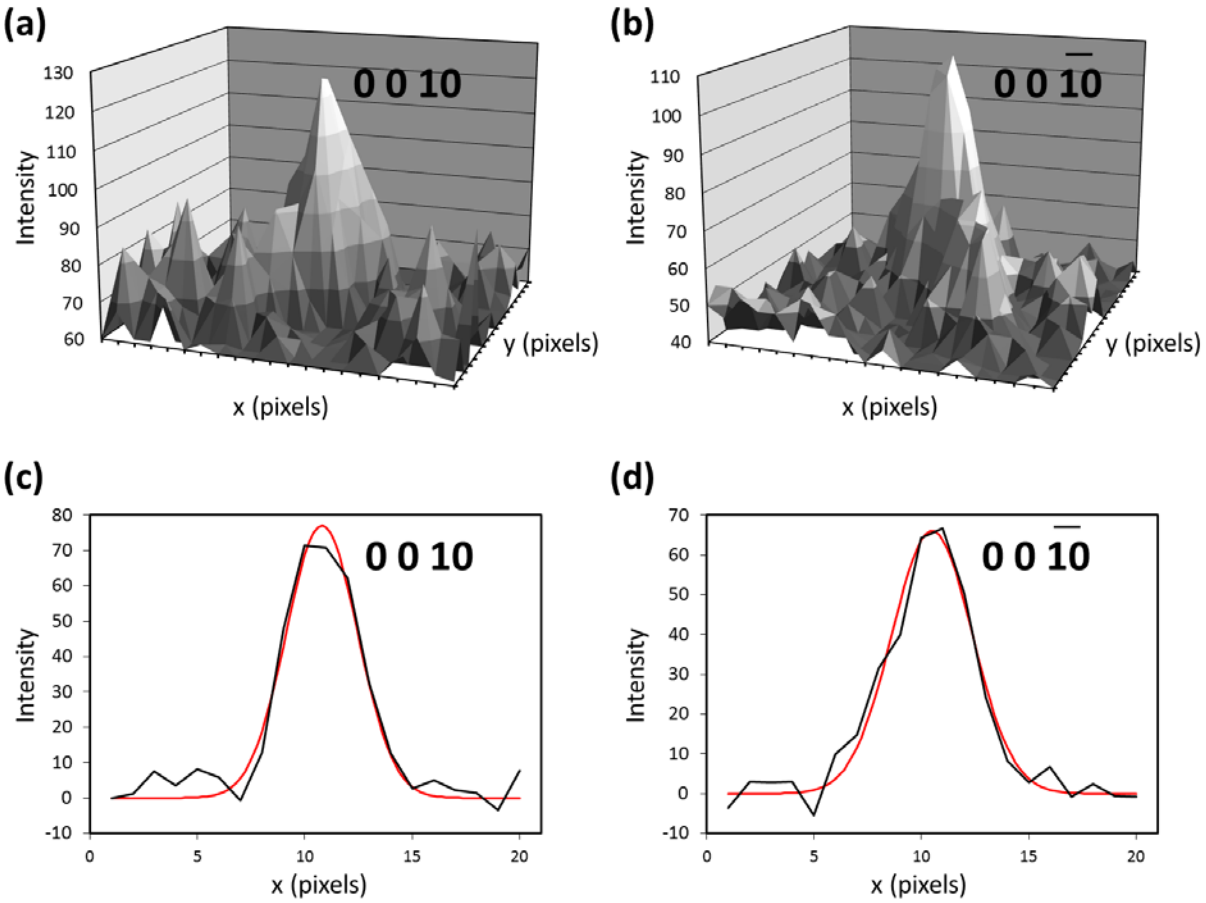

Figure 2 Intensity profiles recorded by CCD detector. (a) 0010 and (b) $00\bar{1}0$ reflections corresponding to reflection conditions of type 00*l* with *l* = 2*n*, which is consistent with the orthorhombic space group *Ibca*. The rocking curves of the (c) 0010 and (d) $00\bar{1}0$ reflections and their profiles fitted to a Gaussian function.

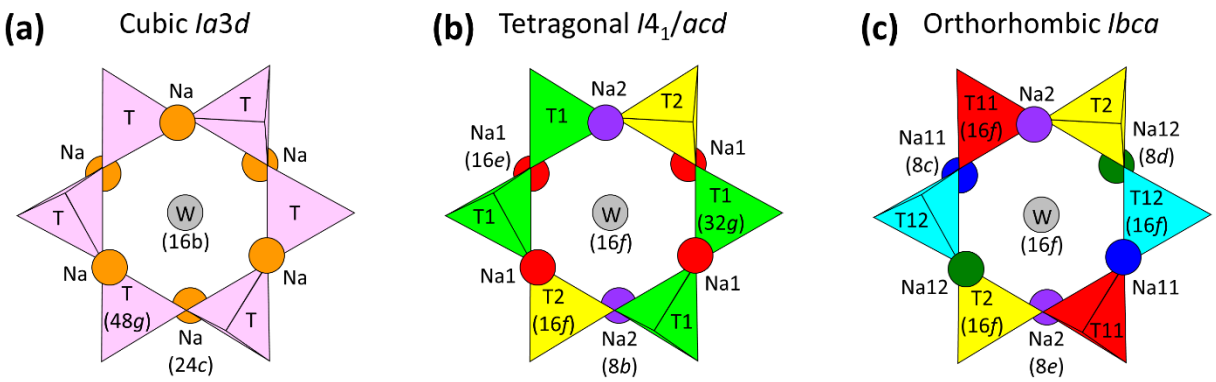

Figure 3 The six-membered ring channel and extra-framework species of analcime viewed along the [111] direction. The site splitting from (a) the cubic analcime with space group *Ia*3*d* to (c) the orthorhombic analcime with space group *Ibca* through (b) the tetragonal space group $I4_1/acd$. The terms in the parentheses denote Wyckoff positions.

Table 1. Representative chemical compositions of analcimes

	ideal	0h	24h	48h
SiO_2	54.58	57.0	57.8	57.0
Al_2O_3	23.16	20.4	19.3	21.0
Na_2O	14.08	11.7	11.7	11.8
		Water contents from thermogravimetry		
H_2O^*	8.18	8.4	8.4	8.4
Total (wt %)	100.00	97.5	97.2	98.2
		Number of cations on the based of 6 oxygen atoms		
Si	2.000	2.12	2.15	2.10
Al	1.000	0.89	0.85	0.91
ΣT	3.000	3.01	3.00	3.02
Na	1.000	0.84	0.85	0.84
H_2O	1.000	1.04	1.04	1.03

Notes:
* The H_2O contents were determined using TG analyses by calculating the weight lost between 100 and 450 °C.

Table 2. Selected X-ray diffraction data and crystallographic information for analcimes

Heating time (h)		0	24	48
Crystal system		Cubic	Orthorhombic	Orthorhombic
Space group		*Ia* 3*d*	*Ibca*	*Ibca*
Lattice parameters	*a* (Å)	13.713(3)	13.727(2)	13.705(2)
	b (Å)		13.707(2)	13.717(2)
	c (Å)		13.707(2)	13.706(2)
Unit cell volume	V (Å^3)	2578.6(10)	2579.0(9)	2576.5(9)
Z		16	16	16
D_{calc} (g/cm^3)		2.226	2.222	2.224
μ (mm^{-1})		0.74	0.73	0.73
$2\theta_{max}$		54.67	56.93	57.12
Reciprocal space range *hkl*		$-19 \le h \le 17$	$-17 \le h \le 18$	$-17 \le h \le 18$
		$-17 \le k \le 17$	$-16 \le k \le 18$	$-13 \le k \le 18$
		$-17 \le l \le 17$	$-18 \le l \le 9$	$-16 \le l \le 17$
No. of collected reflections		7365	7264	7498
Unique reflections, R_{int} (%)		247, 3.34	1540, 2.14	1545, 1.31
Unique reflections with $F_o > 4\sigma(F_o)$		237	1284	1383
No. of parameters		23	115	115
R_1 (%)		1.89	2.39	2.31
wR_2 (%)		5.34	7.33	7.58
GooF		1.158	1.163	1.232
Largest diffraction peak and hole (e$^-$/Å^3)		0.26/-0.17	0.30/-0.32	0.32/-0.30

Table 3. Atomic coordinates, site occupancy parameters, equivalent isotropic, and anisotropic displacement parameters (Å^2).

	Wyckoff position	*x*	*y*	*z*	U_{eq}	Site occupancy	U_{11}	U_{22}	U_{33}	U_{23}	U_{13}	U_{12}
0h												
T	48*g*	0.125	0.16225(2)	0.41225(2)	0.0141(2)	Si:Al = 0.6871:0.3129(14)	0.0137(3)	0.0143(2)	0.0143(2)	0.00098(16)	- 0.00157(11)	0.00157(11)
Na	24*c*	0.125	0	0.25	0.0374(7)	0.6040(14)	0.0362(13)	0.0380(9)	0.0380(9)	- 0.0184(9)	0	0
O	96*h*	0.10449(8)	0.36582(9)	0.21946(7)	0.0328(3)	1.00	0.0369(6)	0.0418(6)	0.0197(5)	- 0.0021(4)	0.0065(5)	- 0.0065(5)
W	16*b*	0.125	0.125	0.125	0.0805(14)	1.00	0.0805(14)	0.0805(14)	0.0805(14)	0.0216(17)	0.0216(17)	0.0216(17)
24h												
*T*11	16*f*	0.12507(4)	0.16228(3)	0.41224(3)	0.01548(13)	Si:Al = 0.618:0.382(2)	0.0160(3)	0.0155(2)	0.0150(2)	0.00119(17)	- 0.00179(17)	0.00130(18)
*T*12	16*f*	0.41228(3)	0.12497(4)	0.16222(3)	0.01588(13)	Si:Al = 0.681:0.319(2)	0.0171(2)	0.0152(2)	0.00154(2)	0.00157(17)	0.00111(17)	- 0.00137(18)
*T*2	16*f*	0.16222(3)	0.41225(3)	0.12500(4)	0.01577(14)	Si:Al = 0.687:0.313(2)	0.0168(2)	0.0156(2)	0.0149(2)	- 0.00155(17)	0.00164(17)	0.00109(17)
Na11	8*c*	0.12520(19)	0	0.25	0.0408(8)	0.591(2)	0.0390(14)	0.0422(14)	0.0411(13)	- 0.0230(10)	0	0
Na12	8*d*	0.25	0.12492(18)	0	0.0416(8)	0.598(2)	0.0447(14)	0.0373(13)	0.0429(13)	0	- 0.0238(10)	0
Na2	8*e*	0	0.25	0.12504(19)	0.0417(8)	0.596(2)	0.0447(14)	0.0432(14)	0.0371(13)	0	0	- 0.0229(11)
O11	16*f*	0.10456(12)	0.36608(12)	0.21960(10)	0.0345(4)	1.00	0.0398 9)	0.0430(9)	0.0205(7)	- 0.0023(6)	0.0066(6)	- 0.0061(7)
O12	16*f*	0.38389(12)	0.14538(12)	0.46953(10)	0.0345(4)	1.00	0.0440(9)	0.0387(9)	0.0208(7)	- 0.0066(6)	0.0021(6)	- 0.0064(7)
O21	16*f*	0.21966(11)	0.10453(12)	0.36596(12)	0.0343(4)	1.00	0.0221(7)	0.0376(9)	0.0433(9)	- 0.0071(7)	- 0.0026(6)	0.0059(6)
O22	16*f*	0.14549(12)	0.46954(11)	0.38404(12)	0.0344(4)	1.00	0.0394(9)	0.0212(7)	0.0425(9)	0.0021(6)	- 0.0064(7)	- 0.0068(6)
O31	16*f*	0.36591(12)	0.21948(11)	0.10445(12)	0.0343(4)	1.00	0.0437(9)	0.0207(7)	0.0385(9)	0.0065(6)	- 0.0063(7)	- 0.0021(6)
O32	16*f*	0.46938(11)	0.38411(12)	0.14547(12)	0.0343(4)	1.00	0.0223(7)	0.0423(9)	0.0383(9)	- 0.0064(7)	- 0.0062(6)	0.0018(6)
W	16*f*	0.1252(2)	0.1249(2)	0.1251(3)	0.0904(9)	1.00	0.091(2)	0.090(2)	0.091(2)	0.0232(16)	0.0222(16)	0.0219(16)

Notes: *W* = water molecule

Table 3. continued.

	Wyckoff position	x	y	z	U_{eq}	Site occupancy	U_{11}	U_{22}	U_{33}	U_{23}	U_{13}	U_{12}
48h												
*T*11	16*f*	0.12498(3)	0.16223(3)	0.41224(3)	0.01348(14)	Si:Al = 0.603:0.397(6)	0.0128(2)	0.0135(2)	0.0141(2)	0.00097(15)	- 0.00173(15)	0.00168(15)
*T*12	16*f*	0.41224(3)	0.12505(3)	0.16226(3)	0.01388(13)	Si:Al = 0.694:0.306(6)	0.0140(2)	0.0133(2)	0.0144(2)	0.00151(15)	0.00099(15)	- 0.00163(15)
*T*2	16*f*	0.16225(3)	0.41224(3)	0.12501(3)	0.01385(13)	Si:Al = 0.687:0.313(6)	0.0139(2)	0.0141(2)	0.0136(2)	- 0.00178(15)	0.00162(15)	0.00095(15)
Na11	8*c*	0.12486(17)	0	0.25	0.0364(7)	0.594(2)	0.0350(12)	0.0375(12)	0.0368(12)	- 0.0181(9)	0	0
Na12	8*d*	0.25	0.12516(17)	0	0.0371(7)	0.602(2)	0.0374(12)	0.0355(12)	0.0383(12)	0	- 0.0184(9)	0
Na2	8*e*	0	0.25	0.12512(17)	0.0370(7)	0.600(2)	0.0380(12)	0.0370(12)	0.0359(12)	0	0	- 0.0194(9)
O11	16*f*	0.10450(11)	0.36577(12)	0.21947(10)	0.0324(3)	1.00	0.0371(7)	0.0406(8)	0.0195(6)	- 0.0024(6)	0.0070(5)	- 0.0075(7)
O12	16*f*	0.38419(12)	0.14557(11)	0.46950(10)	0.0320(3)	1.00	0.0409(8)	0.0355(8)	0.0197(6)	- 0.0069(5)	0.0018(6)	- 0.0072(7)
O21	16*f*	0.21946(10)	0.10455(12)	0.36571(12)	0.0326(3)	1.00	0.0191(6)	0.0376(8)	0.0410(8)	- 0.0067(7)	- 0.0023(6)	0.0067(6)
O22	16*f*	0.14539(12)	0.46948(10)	0.38407(12)	0.0325(3)	1.00	0.0368(8)	0.0191(7)	0.0416(8)	0.0026(6)	- 0.0071(7)	- 0.0065(6)
O31	16*f*	0.36590(12)	0.21952(10)	0.10453(11)	0.0326(3)	1.00	0.0413(8)	0.0189(7)	0.0377(8)	0.0065(5)	- 0.0077(7)	- 0.0018(6)
O32	16*f*	0.46952(10)	0.38396(12)	0.14549(11)	0.0325(3)	1.00	0.0188(6)	0.0417(8)	0.0371(8)	- 0.0074(7)	- 0.0070(5)	0.0020(6)
W	16*f*	0.1250(2)	0.1254(2)	0.1251(2)	0.0809(8)	1.00	0.0807(17)	0.0808(18)	0.0812(18)	0.0246(14)	0.0240(14)	0.0242(14)

Notes: *W* = water molecule

Table 4. Selected bond lengths (Å) in framework *T* sites and extra-framework sites.

0 h		24 h		48 h	
T- O (×2)	1.6430(11)	*T*11- O31	1.6414(15)	*T*11- O12	1.6416(14)
O (×2)	1.6465(11)	O12	1.6416(15)	O31	1.6428(15)
Average	1.645	O32	1.6466(16)	O32	1.6446(15)
		O21	1.6477(16)	O21	1.6460(15)
		Average	1.644	Average	1.644
		*T*12- O11	1.6408(15)	*T*12- O11	1.6415(14)
		O32	1.6453(16)	O32	1.6420(14)
		O22	1.6460(16)	O22	1.6456(15)
		O31	1.6463(16)	O31	1.6458(15)
		Average	1.645	Average	1.644
		*T*2- O22	1.6411(15)	*T*2- O21	1.6424(15)
		O21	1.6425(16)	O22	1.6435(15)
		O12	1.6443(16)	O11	1.6458(15)
		O11	1.6457(16)	O12	1.6467(15)
		Average	1.643	Average	1.645
Na- *W* (×2)	2.4241(5)	Na11- *W* (×2)	2.421(3)	Na11- *W* (×2)	2.427(2)
O (×4)	2.5007(12)	O21 (×2)	2.502(2)	O21 (×2)	2.501(2)
		O32 (×2)	2.502(2)	O32 (×2)	2.502(2)
		Na12- *W* (×2)	2.423(3)	Na12- *W* (×2)	2.424(2)
		O22 (×2)	2.502(2)	O31 (×2)	2.500(2)
		O31 (×2)	2.502(2)	O22 (×2)	2.5030(19)
		Na2- *W* (×2)	2.428(3)	Na2- *W* (×2)	2.420(2)
		O11 (×2)	2.504(2)	O11 (×2)	2.4990(19)
		O12 (×2)	2.505(2)	O12 (×2)	2.5006(19)
W- Na (×3)	2.4241(5)	*W*- Na11	2.421(3)	*W*- Na2	2.420(2)
O (×6)	3.4055(14)	Na12	2.423(3)	Na12	2.424(2)
O (×6)	3.5584(14)	Na2	2.428(3)	Na11	2.427(2)
		O21	3.404(3)	O12	3.401(3)
		O31	3.405(3)	O32	3.403(3)
		O32	3.405(3)	O11	3.403(3)
		O22	3.405(3)	O31	3.404(3)
		O12	3.408(3)	O22	3.408(3)
		O11	3.412(3)	O21	3.412(3)
		O32	3.558(3)	O11	3.553(3)
		O21	3.558(3)	O21	3.555(3)
		O22	3.559(3)	O12	3.556(3)
		O31	3.560(3)	O31	3.557(3)
		O11	3.562(3)	O22	3.561(3)
		O12	3.569(3)	O32	3.567(3)